Article



# Ultrafast Nonlinear Optical Activities of Near-Infrared Aza-BODIPY Derivatives

Can Ren , Shuyu Xiao , Yanyan Cui , Juguang Hu * , Xiaodong Lin * , Tingchao He *

Posted Date: 23 April 2023

doi: 10.20944/preprints202304.0730.v1

Keywords: Near infrared emission; Aza-Bodipy derivatives; Saturable absorption; Nonlinear refraction; Two-photon absorption

*Article*

# Ultrafast Nonlinear Optical Activities of Near-Infrared Aza-BODIPY Derivatives

**Can Ren, Shuyu Xiao, Yanyan Cui, Juguang Hu *, Xiaodong Lin * and Tingchao He ***

Key Laboratory of Optoelectronic Devices and Systems of Ministry of Education and Guangdong Province, College of Physics and Optoelectronic Engineering, Shenzhen University, Shenzhen 518060, China

* Correspondence: hujuguang@szu.edu.cn (J.H.); linxd@szu.edu.cn (X.L.); tche@szu.edu.cn (T.H.)

**Abstract:** The near-infrared (NIR) organic dyes with strong ultrafast nonlinear optical (NLO) activities are of importance for various applications. However, such kinds of dyes are still scarce. In this work, we have compared the NLO properties of two NIR Aza-BODIPY derivatives, in which the strong electron-donating groups, namely 4-(N, N-dimethylamino) phenyl and 1-ethyl-1,2,3,4-tetrahydroquinoline groups, are connected with the cores of Aza-BODIPY. Z-Scan experimental results show that two Aza-BODIPY derivatives exhibit strong saturation absorption and large modulation depth under the excitation of femtosecond pulses at 800 nm. Under 1300 nm excitation, two derivatives exhibit strong nonlinear refraction. In addition, the Aza-BODIPY derivatives also display effective two-photon action cross-sections in the wavelength range of 1200-1600 nm. Based on the experimental results, it is found that 1-ethyl-1,2,3,4-tetrahydroquinoline group can more effectively enhance the NLO properties of Aza-BODIPY derivatives compared with the 4-(N, N-dimethylamino) phenyl group, thus providing new possibilities for the design and development of NIR NLO materials.

**Keywords:** near infrared emission; Aza-BODIPY derivatives; saturable absorption; nonlinear refraction; two-photon absorption

## 1. Introduction

Nonlinear optical (NLO) materials have received much attention due to their application in various optoelectronic devices [1,2]. For example, strong saturable absorption can be used for Q-switching and mode-locking techniques [3,4]. Reverse saturable absorption based optical limiting is considered to be the ideal mechanism for the protection from high intensity laser [5]. The development of fluorescent materials with strong multiphoton absorption (MPA) are desirable for *in vivo* imaging of deep tissue and optical limiting [6,7]. The NLO materials with large nonlinear refraction but weak nonlinear absorption can be used in all-optical switching and optical communications [8,9].

Thus far, various kinds of NLO materials have been reported, including organic molecules [10,11], semiconductor nanocrystals [12], metal nanocrystals [13], organic-inorganic hybrid materials [14] and 2D materials [15]. Among them, organic molecules have a lot of advantages, such as tunable NLO properties through the design of molecular structures, excellent biocompatibility and low fabrication cost [16,17]. Compared with the molecules with visible absorption, near-infrared (NIR) ones have important applications in communication, biological and security [18,19]. For example, the NIR molecules with strong MPA have deep penetration and high resolution in fluorescence imaging [20,21]. In addition, due to the resonance effect, NIR molecules usually have strong nonlinear refraction effects in the communication band, making them to be promising in all-optical switching [22,23].

Boron-dipyrromethene (BODIPY) belongs to a family of organoboron compounds, which displays good photostability and excellent NLO properties [24–26]. As various BODIPY derivatives, Aza-BODIPY derivatives possess superior optical properties, including red-shifted spectra and high molar extinction coefficients [27,28]. Interestingly, through rational molecular design, the absorption and emission spectra of Aza-BODIPY derivatives can shift towards NIR-II biological window (1000-

Preprints (www.preprints.org) | NOT PEER-REVIEWED | Posted: 23 April 2023 doi:10.20944/preprints202304.0730.v1



1350 nm), which are extremely attractive for various applications [29]. Up to now, there are only several papers reporting the NLO properties of Aza-BODIPY derivatives. For example, Chang et al. determined the values of two-photon absorption (2PA) and excited-state absorption (ESA) cross-sections of four Aza-BODIPY derivatives [27]. Liu et al. theoretically investigated 2PA of functionalized Aza-BODIPY derivatives at telecommunication wavelengths [30]. It was also confirmed that Aza-BODIPY derivatives can be used as potential optical limiter [31,32]. However, the study on the NLO properties of Aza-BODIPY derivatives is still very insufficient. For example, there is no literature on the nonlinear refraction and saturation absorption effects of these dyes, which is not conducive to the expansion of relevant applications, or to the understanding of the relationship between NLO properties and molecular structures and excitation wavelength. Therefore, there is an obvious need for further investigation on the influences of the molecular structures and excitation wavelength on the NLO properties of Aza-BODIPY dyes.

In this work, we reported the NLO properties of two Aza-BODIPY derivatives, which are abbreviated as BDP-1 and BDP-2, in which two electron-donating groups 4-(N, N-dimethylamino) phenyl and 1-ethyl-1,2,3,4-tetrahydro- quinoline were connected to the 3 and 5 positions of Aza-BODIPY cores. Actually, Bai et al. reported these two derivatives exhibit effective NIR emission and strong intramolecular charge transfer, implying they may have significant NLO effects [33]. Therefore, we conducted further research on their NLO properties. The experimental results show that both two derivatives exhibit strong saturable absorption at 800 nm. Meanwhile, benefitting from the stronger electron donating ability, Aza-BODIPY-2 possesses larger nonlinear refractive index at 1300 nm and effective two-photon brightness in the wavelength range of 1200 to 1600 nm.

## 2. Results and Discussion

### *2.1. The UV-visible absorption and emission spectra*

Figure 1a shows the structures of two Aza-BODIPY derivatives studied in this work, while their absorption and emission spectra are depicted in Figure 1b. It can be seen that both two samples exhibit two main absorption bands, which are peaking at 690 and 800 nm for BDP-1, and 700 and 860 nm for BDP-2, respectively. Excited by the pulses at 350 nm, the fluorescence emission spectra of two derivatives are peaking at 1000 and 1050 nm, respectively. The photoluminescence quantum yields (PLQYs) were 0.9% and 0.6%, respectively. Importantly, the derivatives emit in the NIR-II biological window. Compared with fluorescence imaging in the NIR-I biological window (650 - 950 nm), NIR-II fluorescence imaging can afford higher spatial resolution, deeper penetration depth into a living body [34]. In addition, two Aza-BODIPY derivatives have large Stokes shifts, *i.e*, 187 nm (53476 $cm^{-1}$) vs 194 nm (51546 $cm^{-1}$), which is an additional advantage for fluorescence imaging in organisms. It was also found that the absorption and emission peaks of BDP-2 shift toward longer wavelengths compared to BDP-1, as a result of the stronger electron-donating ability of 1-ethyl-1,2,3,4-tetrahydroquinoline group in the former [35,36].

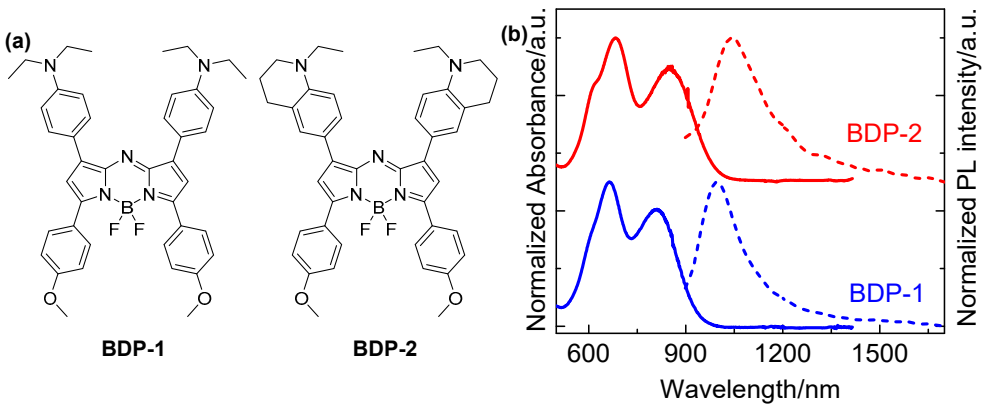

Preprints (www.preprints.org) | NOT PEER-REVIEWED | Posted: 23 April 2023 doi:10.20944/preprints202304.0730.v1



**Figure 1.** (a) Molecular structures of BDP-1 and BDP-2. (b) Normalized absorption and PL spectra of the two derivatives in dimethyl sulfoxide (DMSO) solutions ($1.3 \times 10^{-3}$ M).

*2.2. Ultrafast dynamics*

Next, we investigated the carrier dynamics of two derivatives. Figure 2a and Figure 2c shows the 2D color images of femtosecond-transient absorption (fs-TA) spectra of two derivatives under the excitation wavelength of 800 nm, while their corresponding spectra at selected delay times are depicted in Figure 2b and Figure 2d, respectively. It can be seen that two derivatives exhibit similar signals, in which positive signals appear within the range of 400 - 580 nm, caused by the ESA. Meanwhile, negative signals were observed within the range of 600 - 950 nm. According to the absorption spectrum, we believe these negative signals arise from the ground-state bleaching effect. Two derivatives exhibit negative signals in the wavelength range above 1000 nm, corresponding to the PL spectra. Thus, these negative signals are caused by the stimulated emission. The ESA peaks of two derivatives in the range of 400 - 580 nm exhibit a slight blue shift with increasing time. Possibly, it is caused by the solvent effect in that the polarization degrees of molecules under an excited state will be enhanced [37]. BDP-2 shows a more significant blue shift (10 nm) than that (7 nm) of BDP-1, indicating a higher polarization degree of excitation state that may induce a more significant NLO effect in the former.

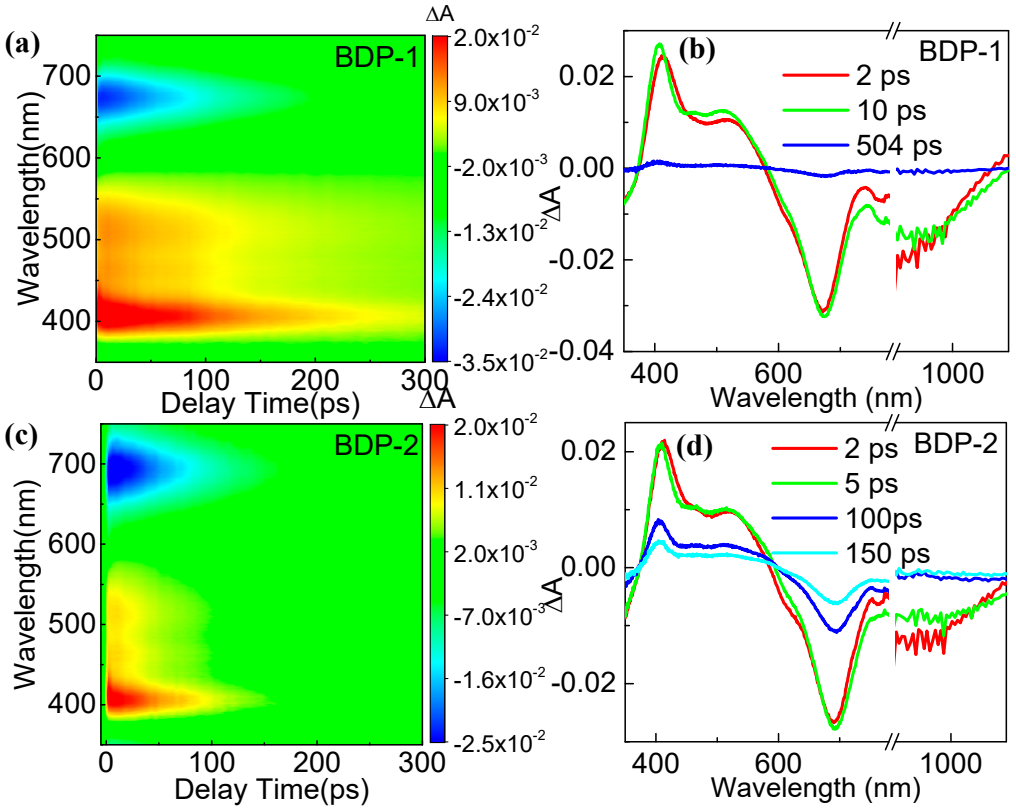


**Figure 2.** Full contour maps of fs-TA spectra under excitation at 800 nm for (a) BDP-1 and (c) BDP-2. Fs-TA spectra at selected delay times for BDP-1 (b) and BDP-2 (d).

*2.3. NLO properties at different excitation wavelengths*

2.3.1. Resonant NLO properties at 800 nm

Because two derivatives possess strong linear absorption below 860 nm, it was expected that strong nonlinear absorption effect may occur within the absorption band. Then, using femtosecond pulses of 800 nm (1000 Hz, 100 fs) as an excitation light source, we measured the open aperture Z-scan data of the DMSO solutions of two derivatives with a concentration of around $1.3 \times 10^{-3}$ M (Figure

Preprints (www.preprints.org) | NOT PEER-REVIEWED | Posted: 23 April 2023 doi:10.20944/preprints202304.0730.v1



3a). The incident light intensity was around 76.4 GW/cm². Under the same incident light intensity, derivatives exhibit strong saturable absorption effect, while no obvious signals were observed in the DMSO solvent.

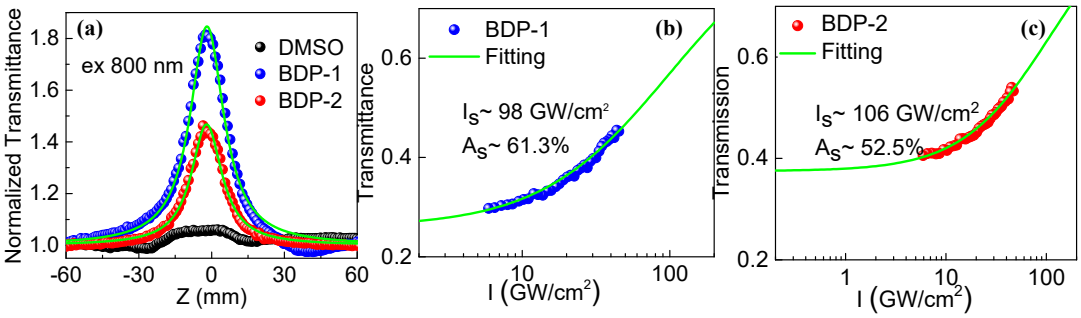


**Figure 3.** (a) open-aperture Z-scan curves of two derivative solutions and pure DMSO solvent at 800 nm. (b, c) nonlinear transmittance curves recorded at 800 nm. The solid lines represent theoretical fitting results according to Equation (3).

In the open-aperture experiment, the simplified expression formula of normalized transmittance can be described as follows [38]:

$$T(z) = 1 - \frac{\beta I_0 L_{eff}}{2\sqrt{2}(1+\frac{z^2}{z_0^2})}, \quad (1)$$

where β (in unit of cm/GW) is the nonlinear absorption coefficients. $I_0$ (in unit of GW/cm²) is the light intensity at the focal point (z=0). $L_{eff}$ (in unit of cm) is the effective length of the sample, which is expressed as $L_{eff}=(1-e^{-\alpha L})/L$, with the linear absorption coefficient $\alpha$ and the physical thickness L. $z_0=k\omega_0/2$ is the diffraction length, in which $k=2\pi/\lambda$ is the wave number and $\omega_0$ is the spot radius at the focal point. By fitting the experimental data with Equation (1), the nonlinear absorption coefficients (β) of BDP-1 and BDP-2 in DMSO solutions can be determined as -0.30 and -0.16 cm/GW. Considering the NLO properties of sample solutions were influenced by the concentration, it will be more objective to compare the intrinsic NLO parameters among different samples according to following equation [39]:

$$x(\text{solution}) = (1-f)x(\text{solvent}) + fx(\text{intrinsic}), \quad (2)$$

in which $x$ (solution) is the total NLO parameters of the sample solution, including nonlinear absorption coefficient, nonlinear refractive index. $f$ is the volume fraction of the derivatives relative to DMSO. $x$ (solvent) is the NLO parameters of DMSO. $x$ (intrinsic) is the intrinsic NLO parameters of the derivatives. As a result, the intrinsic nonlinear coefficients of BDP-1 and BDP-2 were determined, i.e., β (intrinsic) $-1.48 \times 10^4$ and $-8.26 \times 10^3$ cm/GW, respectively. Considering the 4-(N, N-dimethylamino) phenyl group has weaker electron-donating ability than the 1-ethyl-1,2,3,4-tetrahydroquinoline groups, the larger β (intrinsic) of BDP-1 should be caused by its stronger absorption at 800 nm.

To determine the saturable absorption intensity ($I_s$) and modulation depth ($A_s$) of two derivatives, which are two important parameters for the Q-switching or mode-locking of fiber lasers, we measured their transmittances under different excitation intensities, as shown in Figure 3b and Figure 3c. It can be seen that with the increase of incident light intensity their transmittances gradually increase, indicating a saturable absorption effect, which is consistent with the Z-scan data. $I_s$ and $A_s$ of two derivatives were estimated, *i.e.*, 98 GW/cm² and 61.3% for BDP-1 and 106 GW/cm² and 52.5% for BDP-2, according to the following equation [40]:

$$T = 1 - A_s / (1 + I / I_s) - n_s, \quad (3)$$

Preprints (www.preprints.org) | NOT PEER-REVIEWED | Posted: 23 April 2023 doi:10.20944/preprints202304.0730.v1



where I is the input intensity; $A_s$ is the modulation depth; $I_s$ is the saturable absorption; $n_s$ is the nonsaturable loss. In addition, BDP-1 has larger modulation depth and smaller saturable absorption intensity, implying this derivative is more promising for the application in Q-switching or mode-locking of fiber lasers. In order to facilitate comparison, the NLO parameters at 800 nm for two derivatives were compared in Table 1.

**Table 1.** Resonant NLO parameters of samples under 800 nm excitation (1000 Hz, 100 fs).

| Material | $\beta_{Intrinsic}$ (cm/GW) | $I_s$ (GW/cm²) | $A_s$ (%) |
|---|---|---|---|
| BDP-1 | $-1.48 \times 10^4$ | 98 | 61.3 |
| BDP-2 | $-8.26 \times 10^3$ | 106 | 52.5 |

2.3.2. Nonresonant NLO properties at 1300 nm

Considering two derivatives have negligible absorption at 1300 nm, it is interesting to investigate their nonlinear refraction effect and 2PA. From the closed-aperture Z-scan experimental data divided by corresponding open-aperture ones, as shown in Figure 4a, it can be seen that the solutions of two derivatives exhibit a self-defocusing effect, while the DMSO solvent exhibits a self-focusing effect. The experimental data in Figure 4a can be theoretically fitted using following formula [41]:

$$T(z,\Delta\phi_0) = 1 - \frac{4\Delta\phi_0(t)x}{(x^2+9)(x^2+1)}, \quad (4)$$

where $\Delta\Phi_0(t)=k\Delta nL_{eff}$ is the nonlinear phase shift at the focal point and $\Delta n=n_2I_0$. $n_2$ is the nonlinear refractive index, while $x=z/z_0$ is the ratio of the sample position z to the diffraction length $z_0$. As a result, the nonlinear refractive indices of BDP-1 and BDP-2 in derivative solutions, and pure DMSO solvent were determined to as $-3.36 \times 10^{-7}$, $-4.48 \times 10^{-7}$ and $7.71 \times 10^{-7}$ cm²/GW. Although the solution concentrations of two derivatives were much low, their nonlinear refractive indices were only several times smaller than that of carbon disulfide ($n_2 \sim 3.0 \times 10^{-6}$ cm²/GW). With the influence of DMSO solvent subtracted according to Equation (3), the intrinsic nonlinear refractive indices of two derivatives were estimated, i.e., $n_2$ (intrinsic) - $7.60 \times 10^{-3}$ cm²/GW for BDP-1 and $-7.85 \times 10^{-3}$ cm²/GW for BDP-2, respectively. Furthermore, they are even higher than those of organic molecules reported in a lot of NLO materials, including Zn-terpyridine polymer (~ $1.1 \times 10^{-4}$ cm²/GW at 765 nm) [42] and crystalline nickel-p-benzenedicarboxylic acid MOF (Ni-MOF)(~ - $8.9 \times 10^{-7}$ cm²/GW at 1550 nm) [14].

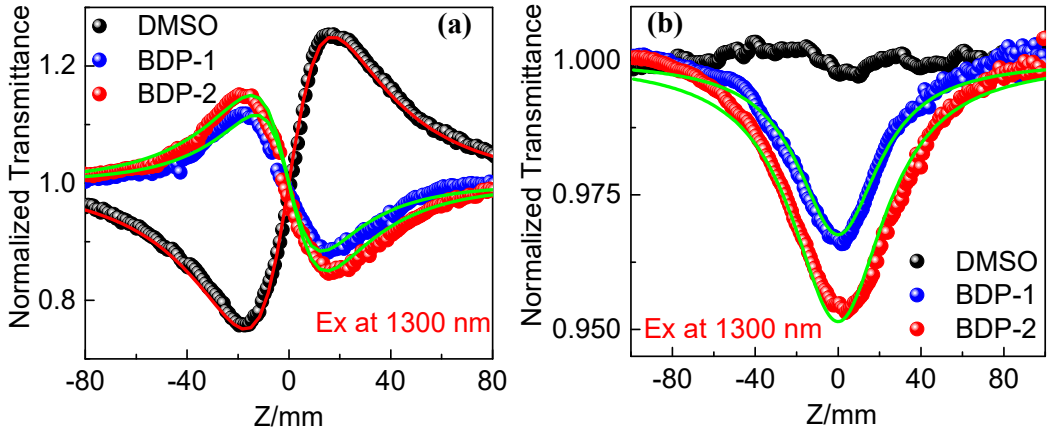


**Figure 4.** (a) Divided Z-scan results of the close-aperture signal by the open-aperture signal at 1300 nm. The solid lines are the fitting results to the data using the Equation (4). (b) open-aperture Z-scan curves of two derivative solutions and pure DMSO solvent at 1300 nm. The incident light intensity is 337 GW/cm².

Preprints (www.preprints.org) | NOT PEER-REVIEWED | Posted: 23 April 2023 doi:10.20944/preprints202304.0730.v1



The open aperture Z-scan data of two derivatives under the excitation of femtosecond pulses of 1300 nm (an excitation light intensity of 337 GW/cm$^2$) are shown in Figure 4b. It can be seen that the signal of solvent can be ignored, and two samples have the smallest transmittances at the focal point, which is caused by 2PA. According to the Equation (1), the 2PA coefficients of BDP-1 and BDP-2 were estimated as 3.35 × 10$^{-3}$ and 4.19 × 10$^{-3}$ cm/GW, respectively. In addition, with the help of Equation (2), the intrinsic 2PA coefficients of two derivatives were determined as 165 and 213 cm GW$^{-1}$. 2PA cross-section ($\sigma_2$) that is in unit of GM, with 1 GM= 10$^{-50}$ cm$^4$ s$^{-1}$ photon$^{-1}$, can be determined according to the following equation [38],

$$\sigma_2 = \frac{\beta h\upsilon}{N_A C_0 \times 10^{-3}}, \tag{5}$$

where h is the Planck's constant in unit of J·s; $\upsilon$ is the incident light frequency in unit of 1/s, $N_A$ is Avogadro's number and $C_0$ is concentration in unit of M/L.

As a result, 2PA cross-sections of BDP-1 and BDP-2 can be estimated as 59 and 77 GM at 800 nm, respectively, as summarized in Table 2. It can be concluded that BDP-2 exhibits larger 2PA cross-section compared to that of BDP-1, as a result of stronger electron-donating ability of the 1-ethyl-1,2,3,4-tetrahydroquinoline groups [43].

To realize the application in all-optical switching, the NLO materials should have strong nonlinear refraction but weak nonlinear absorption. To realize such an application, two Stegeman's figures of merit should satisfy following conditions [44,45]:

$$W = \left|\frac{n_2 I}{\alpha\lambda}\right| > 1, \tag{6}$$

$$T = \left|\frac{\beta\lambda}{n_2}\right| < 1. \tag{7}$$

Since linear absorption of two derivatives are negligible at 1300 nm, their W values are larger than 1. In addition, based on the experimental data, T is estimated as 1.06 for BDP-1 and 0.652 for BDP-2. Therefore, BDP-2 may have potential application in all-optical device applications.

**Table 2.** NLO parameters of derivatives under 1300 nm excitation (1000 Hz, 100 fs).

| Material | $n_2$ (Intrinsic) (cm$^2$/GW) | β (Intrinsic) (cm/GW) | $\sigma_2$ (GM) |
|---|---|---|---|
| BDP-1 | -7.60 × 10$^{-3}$ | 165 | 59 |
| BDP-2 | -7.85 × 10$^{-3}$ | 213 | 77 |

Meanwhile, in order to avoid the influence of linear absorption, we measured the PL spectra of two derivatives under 1400 nm excitation, which are peaking at 1000 and 1060 nm, respectively, as shown in Figure 5a. The spectra are similar to those under single-photon excitation, indicating that the same emission states are involved in two cases. The inset shows the relationship between the PL intensity and excitation power. The slopes around 2 for the best-fitting straight lines on logarithmic scales indicate the occurrence of 2PA. We repeated Z-scan measurements at different wavelengths and obtained their 2PA cross-sections within the range of 1200 - 1600 nm. The molecular probes with large 2PA action cross-sections (the production of a 2PA cross section and PLQY), which is also called two-photon fluorescence brightness, will be beneficial for the two-photon bioimaging. Therefore, 2PA action cross-sections of two derivatives at different wavelengths are calculated and presented in Figure 5b. The moderate 2PA action cross-sections of BDP-2 and PL emission in NIR-II window make it to be promising in deep-tissue bioimaging.

Preprints (www.preprints.org) | NOT PEER-REVIEWED | Posted: 23 April 2023 doi:10.20944/preprints202304.0730.v1



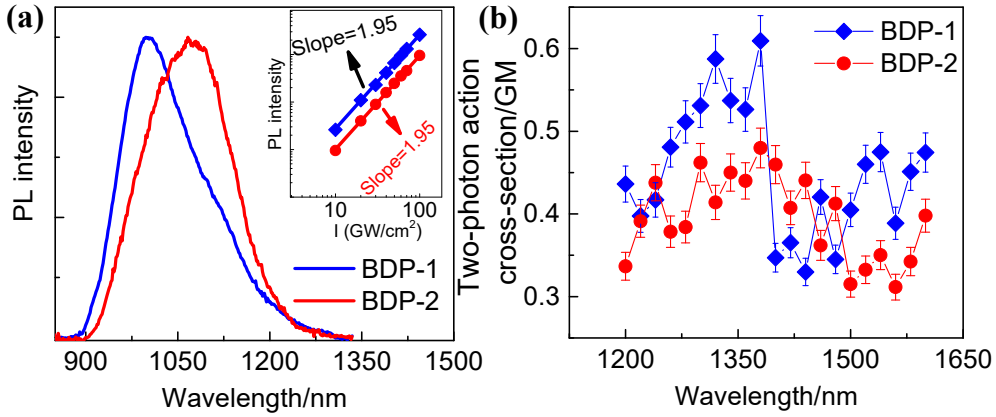


**Figure 5.** (a) Two-photon excited PL spectra of two derivatives. Inset: the relationship between PL intensity and excitation power. (b) 2PA action cross-sections of two samples at different wavelengths.

## 3. Experimental Section

### *3.1. Synthesis of Aza-BODIPY derivatives*

The detailed synthesis procedures were described in Ref. 34. Briefly, BDP-1 or BDP-2 were designed by introducing 4-(N, N-dimethylamino) phenyl or 1-ethyl-1,2,3,4-tetrahydroquinolinyl into the 3 and 5 positions of aza-BODIPY core as electron-donating groups, respectively. In addition, the electron-rich 4-anisoly was incorporated to the 1 and 7 positions of electron-withdrawing aza-BODIPY core. As a result, both BDP-1 and BDP-2 possess a D-A-D structure. Consequently, a metallic brown solid (yield: 90%) was obtained for BDP-1, while a metallic brown solid (yield: 90%) was obtained for BDP-2.

### *3.2. Linear optical measurements*

The UV-visible absorption spectra of the Aza-BODIPY derivatives were measured using an ultraviolet-visible-NIR spectrophotometer (Lambda 950). Meanwhile, PL spectra and PLQYs were determined with a FluoroSENS fluorescence spectrometer equipped with a 150 W xenon lamp and an integrating sphere accessory. During the measurements, the samples were dissolved in DMSO, and the solutions obtained with a concentration of $1.3 \times 10^{-5}$ M were filled into 1 cm cuvettes.

### *3.3. fs-TA spectrum*

During the measurements, the pump pulses at 800 nm were generated with an optical parametric amplifier system (Spectra-physics Spitfire Ace) that was combined with TOPAS. Meanwhile, the probe pulses in the wavelength ranges of 350 – 750 nm or 950 – 1200 nm were generated by a YAG crystal or $CaF_2$ crystal, respectively. The sample solutions were filled in quartz liquid cells with a thickness of 1 mm. To eliminate any contribution from coherent artifacts, the linear polarization of the pump pulse was adjusted to be perpendicular to that of the probe pulse. Pump-induced changes of transmission ($\Delta T/T$) of the probe beam were monitored using a monochromator/photomultiplier configuration with lock-in detection.

### *3.4. NLO characterizations*

The NLO parameters of two derivatives at 800 nm and 1200-1600 nm were determined using Z-scan technique [41]. Because of the ultrashort pulse width (100 fs) and low repetition frequency (1000 Hz) of the excitation light, the thermal effect (occurring within the ns range) can be neglected in the measurements of NLO parameters [46,47]. Before conducting the measurement, the $CS_2$ was used as reference to calibrate the Z-scan system, and the obtained $n_2$ value of $CS_2$ (~$4.53 \times 10^{-6}$ cm²/GW) is consistent with that in previous literature [48], confirming the reliability of our Z-scan experiment. Generally, $n_2$ and $\beta$ can be obtained by the measurement of the normalized transmittance for the

closed and open aperture versus sample position. If there is nonlinear absorption existing in the samples, the closed transmittance is affected by both $n_2$ and β. The determination of $n_2$ is less straightforward from the closed aperture Z-scan curve. It is necessary to separate the effect of nonlinear absorption by dividing closed-aperture Z-scan experimental data by corresponding open-aperture ones. For the I-scan measurements, the samples were fixed at the focal point, and the incident light intensity was continuously changed by computer-controlled electric attenuator. For the measurements of multiphoton excited PL spectra, the femtosecond pulses with wavelengths from 1200 to 1600 nm were used as the excitation source and the signals were vertically collected with a compact spectrometer (NIRQuest 512).

## 4. Conclusions

In this work, we studied the NLO properties of two Aza-BODIPY derivatives, with their PL emission wavelengths in NIR-II window. The experimental results indicate that two derivatives possess strong saturable absorption and large modulation depth under the excitation at 800 nm, while they exhibit strong nonlinear refraction at 1300 nm. Interestingly, two derivatives have moderate 2PA action cross-sections in the wavelength range of 1200-1600 nm. The excellent NLO properties of the Aza-BODIPY derivatives implied they are promising for various application, including Q-switching or mode-locking of pulse lasers, all-optical switching, deep tissue bioimaging in NIR-II window.

**Author Contributions:** Conceptualization, T.H.; methodology, validation, formal analysis, C.R. and S.X.; investigation, C.R., S.X. and Y.C.; resources, T.H.; data curation, writing—original draft preparation, C.R. and S.X.; writing—review and editing, and visualization, C.R. and T.H.; supervision, X.L., J.H. and T.H.; project administration, T.H.; funding acquisition, C.R. and T.H.. All authors have read and agreed to the published version of the manuscript.

**Funding:** This research was funded by the Guangdong Basic and Applied Basic Research Foundation (2022A1515011246), the Science and Technology Planning Project of Shenzhen Municipality (JCYJ20210324094414039), and the China Postdoctoral Science Foundation (2021TQ0214).

**Conflicts of Interest:** The authors declare no conflict of interest.

## References

1. Nguyen, V.-N.; Ha, J.; Cho, M.; Li, H.; Swamy, K.M.K.; Yoon, J. Recent developments ofBODIPY-based colorimetric and fluorescent probes for the detection of reactive oxygen/nitrogen species and cancer diagnosis. *Coord. Chem. Rev.* **2021**, *439*, 213936, doi:https://doi.org/10.1016/j.ccr.2021.213936.
2. Ghanavatkar, C.W.; Mishra, V.R.; Sekar, N. Review of NLOphoric azo dyes – Developments in hyperpolarizabilities in last two decades. *Dyes Pigm.* **2021**, *191*, 109367, doi:https://doi.org/10.1016/j.dyepig.2021.109367.
3. Wang, W.; Yue, W.; Liu, Z.; Shi, T.; Du, J.; Leng, Y.; Wei, R.; Ye, Y.; Liu, C.; Liu, X.; et al. Ultrafast Nonlinear Optical Response in Plasmonic 2D Molybdenum Oxide Nanosheets for Mode-Locked Pulse Generation. *Adv. Opt. Mater.* **2018**, *6*, 1700948, doi:https://doi.org/10.1002/adom.201700948.
4. Zhang, C.; Ouyang, H.; Miao, R.; Sui, Y.; Hao, H.; Tang, Y.; You, J.; Zheng, X.; Xu, Z.; Cheng, X.a.; et al. Anisotropic Nonlinear Optical Properties of a SnSe Flake and a Novel Perspective for the Application of All‐Optical Switching. *Adv. Opt. Mater.* **2019**, *7*, 1900631, doi: https://doi.org/10.1002/adom.201900631.
5. Tian, Y.-B.; Li, Q.-H.; Wang, Z.; Gu, Z.-G.; Zhang, J. Coordination-Induced Symmetry Breaking on Metal-Porphyrinic Framework Thin Films for Enhanced Nonlinear Optical Limiting. *Nano Lett.* **2023**, *23*, 3062-3069, doi:https://doi.org/10.1021/acs.nanolett.3c00635.
6. Fang, F.; Yuan, Y.; Wan, Y.; Li, J.; Song, Y.; Chen, W.-C.; Zhao, D.; Chi, Y.; Li, M.; Lee, C.-S.; et al. Near-Infrared Thermally Activated Delayed Fluorescence Nanoparticle: A Metal-Free Photosensitizer for Two-Photon-Activated Photodynamic Therapy at the Cell and Small Animal Levels. *Small* **2022**, *18*, 2106215, doi:https://doi.org/10.1002/smll.202106215.
7. Yu, M.; Okawachi, Y.; Griffith, A.G.; Picqué, N.; Lipson, M.; Gaeta, A.L. Silicon-chip-based mid-infrared dual-comb spectroscopy. *Nat. Commun.* **2018**, *9*, 1869, doi:https://doi.org/10.1038/s41467-018-04350-1.

8. Chen, J.; Hu, C.-L.; Kong, F.; Mao, J.-G. High-Performance Second-Harmonic-Generation (SHG) Materials: New Developments and New Strategies. *Acc. Chem. Res.* **2021**, *54*, 2775-2783, doi:https://doi.org/10.1021/acs.accounts.1c00188.
9. Beharry, A.A.; Woolley, G.A. Azobenzene photoswitches for biomolecules. *Chem. Soc. Rev.* **2011**, *40*, 4422-4437, doi:http://dx.doi.org/10.1039/C1CS15023E.
10. Ren, C.; Xiao, S.; Li, J.; Ma, L.; Chen, R.; Ye, C.; Gao, Y.; Su, C.; He, T. Large Nonlinear Optical Activity of a Near-infrared-absorbing Bithiophene-based Polymer with a Head-to-head Linkage. *Chemistry – An Asian Journal* **2021**, *16*, 309-314, doi:https://doi.org/10.1002/asia.202001311.
11. Achelle, S.; Verbitskiy, E.V.; Fecková, M.; Bureš, F.; Barsella, A.; Robin-le Guen, F. V-Shaped Methylpyrimidinium Chromophores for Nonlinear Optics. *ChemPlusChem* **2021**, *86*, 758-762, doi:https://doi.org/10.1002/cplu.202100081.
12. Ren, C.; Hu, D.; Cui, Y.; Chen, P.; Xu, X.; Cheng, J.; He, T. Ag-doped InP/ZnS quantum dots for type-I photosensitizers. *Chem. Commun.* **2023**, *59*, 2311-2314, doi:http://dx.doi.org/10.1039/D2CC06119H.
13. Li, J.; Ren, C.; Qiu, X.; Lin, X.; Chen, R.; Yin, C.; He, T. Ultrafast optical nonlinearity of blue-emitting perovskite nanocrystals. *Photonics Res.* **2018**, *6*, 554-559, doi:https://doi.org/10.1364/PRJ.6.000554.
14. Jiang, X.; Zhang, L.; Liu, S.; Zhang, Y.; He, Z.; Li, W.; Zhang, F.; Shi, Y.; Lü, W.; Li, Y.; et al. Ultrathin Metal–Organic Framework: An Emerging Broadband Nonlinear Optical Material for Ultrafast Photonics. *Adv. Opt. Mater.* **2018**, *6*, 1800561, doi:https://doi.org/10.1002/adom.201800561.
15. Yu, J.; Kuang, X.; Li, J.; Zhong, J.; Zeng, C.; Cao, L.; Liu, Z.; Zeng, Z.; Luo, Z.; He, T.; et al. Giant nonlinear optical activity in two-dimensional palladium diselenide. *Nat. Commun.* **2021**, *12*, 1083, doi:https://doi.org/10.1038/s41467-021-21267-4.
16. Wen, K.; Tan, H.; Peng, Q.; Chen, H.; Ma, H.; Wang, L.; Peng, A.; Shi, Q.; Cai, X.; Huang, H. Achieving Efficient NIR-II Type-I Photosensitizers for Photodynamic/Photothermal Therapy upon Regulating Chalcogen Elements. *Adv. Mater.* **2022**, *34*, 2108146, doi:https://doi.org/10.1002/adma.202108146.
17. Liu, J.; Ouyang, C.; Huo, F.; He, W.; Cao, A. Progress in the enhancement of electro-optic coefficients and orientation stability for organic second-order nonlinear optical materials. *Dyes Pigm.* **2020**, *181*, 108509, doi:https://doi.org/10.1016/j.dyepig.2020.108509.
18. Wang, S.; Chen, H.; Liu, J.; Chen, C.; Liu, B. NIR‐II Light Activated Photosensitizer with Aggregation‐Induced Emission for Precise and Efficient Two‐Photon Photodynamic Cancer Cell Ablation. *Adv. Funct. Mater.* **2020**, *30*, doi: https://doi.org/10.1002/adfm.202002546.
19. Yu, P.; Yan, K.; Wang, S.; Yao, C.; Lei, Z.; Tang, Y.; Zhang, F. NIR-II Dyad-Doped Ratiometric Nanosensor with Enhanced Spectral Fidelity in Biological Media for In Vivo Biosensing. *Nano Lett.* **2022**, *22*, 9732-9740, doi:https://doi.org/10.1021/acs.nanolett.2c04084.
20. Liu, P.; Mu, X.; Zhang, X.-D.; Ming, D. The Near-Infrared-II Fluorophores and Advanced Microscopy Technologies Development and Application in Bioimaging. *Bioconjugate Chem.* **2020**, *31*, 260-275, doi:https://doi.org/10.1021/acs.bioconjchem.9b00610.
21. Guo, X.; Tang, B.; Wu, Q.; Bu, W.; Zhang, F.; Yu, C.; Jiao, L.; Hao, E. Engineering BODIPY-based near-infrared nanoparticles with large Stokes shifts and aggregation-induced emission characteristics for organelle specific bioimaging. *J. Mater. Chem. B* **2022**, *10*, 5612-5623, doi:http://dx.doi.org/10.1039/D2TB00921H.
22. Liu, B.-W.; Jiang, X.-M.; Zeng, H.-Y.; Guo, G.-C. [ABa2Cl][Ga4S8] (A = Rb, Cs): Wide-Spectrum Nonlinear Optical Materials Obtained by Polycation-Substitution-Induced Nonlinear Optical (NLO)-Functional Motif Ordering. *J. Am. Chem. Soc.* **2020**, *142*, 10641-10645, doi:https://doi.org/10.1021/jacs.0c04738.
23. Kang, D.; Li, R.; Cao, S.; Sun, M. Nonlinear optical microscopies: physical principle and applications. *Appl. Spectrosc. Rev.* **2021**, *56*, 52-66, doi:https://doi.org/10.1080/05704928.2020.1728295.
24. Li, K.; Duan, X.; Jiang, Z.; Ding, D.; Chen, Y.; Zhang, G.-Q.; Liu, Z. J-aggregates of meso-[2.2]paracyclophanyl-BODIPY dye for NIR-II imaging. *Nat. Commun.* **2021**, *12*, 2376, doi:https://doi.org/10.1038/s41467-021-22686-z.
25. Ren, C.; Deng, X.; Hu, W.; Li, J.; Miao, X.; Xiao, S.; Liu, H.; Fan, Q.; Wang, K.; He, T. A near-infrared I emissive dye: toward the application of saturable absorber and multiphoton fluorescence microscopy in the deep-tissue imaging window. *Chem. Commun.* **2019**, *55*, 5111-5114, doi:http://dx.doi.org/10.1039/C9CC02120E.
26. Chang, H.-J.; Bondar, M.V.; Munera, N.; David, S.; Maury, O.; Berginc, G.; Le Guennic, B.; Jacquemin, D.; Andraud, C.; Hagan, D.J.; et al. Femtosecond Spectroscopy and Nonlinear Optical Properties of aza-

BODIPY Derivatives in Solution. *Chem.-Eur. J.* **2022**, *28*, e202104072, doi:https://doi.org/10.1002/chem.202104072.

27. Merkes, J.M.; Lammers, T.; Kancherla, R.; Rueping, M.; Kiessling, F.; Banala, S. Tuning Optical Properties of BODIPY Dyes by Pyrrole Conjugation for Photoacoustic Imaging. *Adv. Opt. Mater.* **2020**, *8*, 1902115, doi:https://doi.org/10.1002/adom.201902115.
28. Gurubasavaraj, P.M.; Sajjan, V.P.; Muñoz-Flores, B.M.; Jiménez Pérez, V.M.; Hosmane, N.S. Recent Advances in BODIPY Compounds: Synthetic Methods, Optical and Nonlinear Optical Properties, and Their Medical Applications. *Molecules* **2022**, *27*, 1877, doi:https://doi.org/10.3390/molecules27061877.
29. Jiang, X.; Zhang, T.; Sun, C.; Meng, Y.; Xiao, L. Synthesis of aza-BODIPY dyes bearing the naphthyl groups at 1,7-positions and application for singlet oxygen generation. *Chin. Chem. Lett.* **2019**, *30*, 1055-1058, doi:https://doi.org/10.1016/j.cclet.2019.02.016.
30. Liu, X.; Zhang, J.; Li, K.; Sun, X.; Wu, Z.; Ren, A.; Feng, J. New insights into two-photon absorption properties of functionalized aza-BODIPY dyes at telecommunication wavelengths: a theoretical study. *Phys. Chem. Chem. Phys.* **2013**, *15*, 4666-4676, doi:http://dx.doi.org/10.1039/C3CP44435J.
31. David, S.; Chang, H.-J.; Lopes, C.; Brännlund, C.; Le Guennic, B.; Berginc, G.; Van Stryland, E.; Bondar, M.V.; Hagan, D.; Jacquemin, D.; et al. Benzothiadiazole-Substituted Aza-BODIPY Dyes: Two-Photon Absorption Enhancement for Improved Optical Limiting Performances in the Short-Wave IR Range. *Chem.-Eur. J.* **2021**, *27*, 3517-3525, doi:https://doi.org/10.1002/chem.202004899.
32. David, S.; Chateau, D.; Chang, H.-J.; Karlsson, L.H.; Bondar, M.V.; Lopes, C.; Le Guennic, B.; Jacquemin, D.; Berginc, G.; Maury, O.; et al. High-Performance Optical Power Limiting Filters at Telecommunication Wavelengths: When Aza-BODIPY Dyes Bond to Sol–Gel Materials. *J. Phys. Chem. C* **2020**, *124*, 24344-24350, doi:https://doi.org/10.1021/acs.jpcc.0c08006.
33. Bai, L.; Sun, P.; Liu, Y.; Zhang, H.; Hu, W.; Zhang, W.; Liu, Z.; Fan, Q.; Li, L.; Huang, W. Novel aza-BODIPY based small molecular NIR-II fluorophores for in vivo imaging. *Chem. Commun.* **2019**, *55*, 10920-10923, doi:http://dx.doi.org/10.1039/C9CC03378E.
34. Miao, X.F.; Tao, H.; Hu, W.; Pan, Y.; Fan, Q.; Huang, W. Elucidating the excited-state dynamics behavior in near-infrared Bodipy dye and aggregates toward biophotonics. *Sci. China Chem.* **2020**, *63*, 1075-1081, doi:https://doi.org/10.1007/s11426-020-9731-0.
35. Tekin, S.; Küçüköz, B.; Yılmaz, H.; Sevinç, G.; Hayvalı, M.; Gul Yaglioglu, H.; Elmali, A. Enhancement of two photon absorption properties by charge transfer in newly synthesized aza-boron-dipyrromethene compounds containing triphenylamine, 4-ethynyl-N,N-dimethylaniline and methoxy moieties. *J. Photochem. Photobiol., A* **2013**, *256*, 23-28, doi:https://doi.org/10.1016/j.jphotochem.2013.02.002.
36. Karatay, A.; Yılmaz, H.; Yildiz, E.A.; Sevinç, G.; Hayvali, M.; Boyacioglu, B.; Unver, H.; Elmali, A. Two-photon absorption and triplet excited state quenching of near-IR region aza-BODIPY photosensitizers via a triphenylamine moiety despite heavy bromine atoms. *Phys. Chem. Chem. Phys.* **2022**, *24*, 25495-25505, doi:http://dx.doi.org/10.1039/D2CP02960J.
37. Chang, Y.J.; Castner, E.W. Intermolecular Dynamics of Substituted Benzene and Cyclohexane Liquids, Studied by Femtosecond Nonlinear-Optical Polarization Spectroscopy. *The Journal of Physical Chemistry* **1996**, *100*, 3330-3343, doi:https://doi.org/10.1021/jp952073o.
38. Mushtaq, A.; Kushavah, D.; Ghosh, S.; Pal, S.K. Nonlinear optical properties of benzylamine lead(II) bromide perovskite microdisks in femtosecond regime. *Appl. Phys. Lett.* **2019**, *114*, 051902, doi:https://doi.org/10.1063/1.5082376.
39. He, G.S.; Zhu, J.; Baev, A.; Samoć, M.; Frattarelli, D.L.; Watanabe, N.; Facchetti, A.; Ågren, H.; Marks, T.J.; Prasad, P.N. Twisted π-System Chromophores for All-Optical Switching. *J. Am. Chem. Soc.* **2011**, *133*, 6675-6680, doi:https://doi.org/10.1021/ja1113112.
40. Dong, N.; Li, Y.; Zhang, S.; McEvoy, N.; Gatensby, R.; Duesberg, G.S.; Wang, J. Saturation of Two-Photon Absorption in Layered Transition Metal Dichalcogenides: Experiment and Theory. *ACS Photonics* **2018**, *5*, 1558-1565, doi:https://doi.org/10.1021/acsphotonics.8b00010.
41. Sheikbahae, M.; Said, A.A.; Wei, T.H.; Hagan, D.J.; Vanstryland, E.W. Sensitive measurement of optical nonlinearities using a single beam. *IEEE J. Quantum Electron.* **1990**, *26*, 760-769, doi:https://doi.org/10.1109/3.53394.
42. He, T.; Too, P.C.; Chen, R.; Chiba, S.; Sun, H. Concise Synthesis and Two-Photon-Excited Deep-Blue Emission of 1,8-Diazapyrenes. *Chem.-Asian J.* **2012**, *7*, 2090-2095, doi:https://doi.org/10.1002/asia.201200192.

43. Yager, K.G.; Barrett, C.J. Novel photo-switching using azobenzene functional materials. *J. Photochem. Photobiol., A* **2006**, *182*, 250-261, doi:https://doi.org/10.1016/j.jphotochem.2006.04.021.
44. Mizrahi, V.; DeLong, K.W.; Stegeman, G.I.; Saifi, M.A.; Andrejco, M.J. Two-photon absorption as a limitation to all-optical switching. *Opt. Lett.* **1989**, *14*, 1140-1142, doi:https://doi.org/10.1364/OL.14.001140.
45. Zhao, P.; Reichert, M.; Hagan, D.J.; Van Stryland, E.W. Dispersion of nondegenerate nonlinear refraction in semiconductors. *Opt. Express* **2016**, *24*, 24907-24920, doi:https://doi.org/10.1364/OE.24.024907.
46. Kovsh, D.I.; Hagan, D.J.; Stryland, E.W.V. Numerical modeling of thermal refraction in liquids in the transient regime. *Opt. Express* **1999**, *4*, 315-327, doi:https://doi.org/10.1364/OE.4.000315.
47. Li, X.; Hu, K.; Lyu, B.; Zhang, J.; Wang, Y.; Wang, P.; Xiao, S.; Gao, Y.; He, J. Enhanced Nonlinear Optical Response of Rectangular MoS2 and MoS2/TiO2 in Dispersion and Film. *J. Phys. Chem. C* **2016**, *120*, 18243-18248, doi:https://doi.org/10.1021/acs.jpcc.6b04974.
48. Ganeev, R.A.; Ryasnyansky, A.I.; Baba, M.; Suzuki, M.; Ishizawa, N.; Turu, M.; Sakakibara, S.; Kuroda, H. Nonlinear refraction in $CS_2$. *Appl. Phys. B* **2004**, *78*, 433-438, doi:https://doi.org/10.1007/s00340-003-1389-y.